

EScheme: Vision-and-Language Navigation with Episodic Scene Memory

Qi Zheng¹, Daqing Liu², Chaoyue Wang², Jing Zhang², Dadong Wang³, and Dacheng Tao^{1,2}

¹University of Sydney, NSW 2008, Australia

²JD Explore Academy

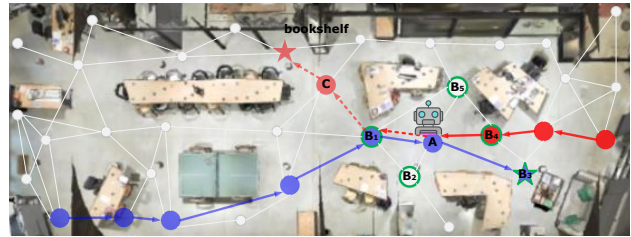
³DATA61, CSIRO, NSW 2122, Australia

Abstract

Vision-and-language navigation (VLN) simulates a visual agent that follows natural-language navigation instructions in real-world scenes. Existing approaches have made enormous progress in navigation in new environments, such as beam search, pre-exploration, and dynamic or hierarchical history encoding. To balance generalization and efficiency, we resort to memorizing visited scenarios apart from the ongoing route while navigating. In this work, we introduce a mechanism of Episodic Scene memory (ESceme) for VLN that wakes an agent’s memories of past visits when it enters the current scene. The episodic scene memory allows the agent to envision a bigger picture of the next prediction. In this way, the agent learns to make the most of currently available information instead of merely adapting to the seen environments. We provide a simple yet effective implementation by enhancing the observation features of candidate nodes during training. We verify the superiority of ESceme on three VLN tasks, including short-horizon navigation (R2R), long-horizon navigation (R4R), and vision-and-dialog navigation (CVDN), and achieve a new state-of-the-art. Code is available: <https://github.com/qizhust/esceme>.

1 Introduction

Vision-and-language navigation (VLN) is firstly defined in [3] towards the goal of a robot carrying out general verbal instructions. VLN requires an agent to follow natural-language instructions based on what it sees and focuses on executing the instructions in previously unseen environments. With the advent of breakthroughs in vision and language, VLN attracts more and more attention recently and develops tasks in various settings, such as fine-grained and short-horizon navigation (e.g. R2R [3] and RxR [20]), long-horizon navigation (e.g. R4R [17]), vision-and-dialogue



Instruction 1: Walk toward and past the ping pong table. Continue in that direction until you reach the sofa with two green pillows. Stop in front of the table that is in front of that sofa.

Instruction 2: Walk through the office past the work tables. Go to the right and stop next to the white bookshelf outside the conference room.

Figure 1. The **blue** trajectory shows an agent carrying out instruction 1. The next time, the agent enters this scene to conduct the second instruction along the **red** path. ESceme allows it to recall the visited nodes (i.e., the **blue** ones) at where it is standing (A) and choose the neighboring node B₁ that will see “the white bookshelf” in one more step at C. Finally, it navigates towards the **red** dash route and reaches the target.

navigation (e.g. CVDN [35]), and navigation with high-level instructions (e.g. REVERIE [31]).

Compared with vision-and-language tasks such as visual question answering [4] and visual captioning [9, 42], changing observations after a VLN agent conducts each action increases the difficulty of decision-making. History encoding algorithms alleviate this issue by tracking past decisions along the trajectory, such as hierarchical encoder [7], structured memory [36], and dual-scale encoding [8]. Another severer challenge comes from generalizing to new environments with more significant differences in observations. Interaction with the novel embodiment increases deviation accumulation in navigation. Thus, a pretraining-finetuning paradigm has been introduced to VLN to capture more general representations [14, 16, 7, 32], and various data augmentation techniques are also developed [13, 34, 21]. An-

other branch of endeavor towards this goal exploits different strategies to navigate the new environment, which include modified beam search [13] and pre-exploration in unseen data [38, 34, 27, 44]. Although the strategies notably improve VLN performance in unseen environments, they are too expensive for a deployed robot. Specifically, beam search significantly extends navigation routes. Pre-exploration takes extra time before conducting the given instruction and finetunes the agent with auxiliary objectives, which is impractical on terminal devices.

In this work, we propose a navigation mechanism with Episodic Scene memory (ESceme) to balance generalization and efficiency. ESceme requires no extra annotations or heavy computation and is agent-agnostic. We update the scene memory during navigation, which envisions the agent seeing a bigger picture in each decision via candidate enhancing. This way, the agent learns to make the most use of available information instead of merely adapting to current observations. Then during inference, it predicts actions with the progressively completed memory. A demonstration shows in Figure 1. When carrying out an instruction at Location A, the agent is to select one from the adjacent nodes B_1 - B_5 to navigate. It recalls the episodic scene memory, i.e. the blue route, and chooses Node B_1 that will see “*the white bookshelf*” in one more step at C.

We verify the superiority of ESceme in three VLN tasks, including short-horizon navigation with fine-grained instruction (R2R), long-horizon navigation (R4R), and vision-and-dialog navigation (CVDN). Our method improves on all three datasets regarding navigation in new environments. We find that ESceme notably benefits navigation with longer routes (R4R and CVDN), promoting both successful reaching and path fidelity. Our method achieves the highest Goal Progress in the CVDN challenge. Besides a fair comparison with existing approaches under a single run, we test the performance with an approximately complete memory, where the agent fully updates its scene memory in the first round of navigation over all the episodes. We denote this setting as *infer twice*, which serves as the upper bound of ESceme. We observe a slightly further improvement in *infer twice*, which indicates that the agent has already learned effective navigation with partially completed scene memory. We hope this work can inspire further explorations in modeling episodic scene memory for VLN.

It is worth noting that it is fair to compare ESceme with its counterparts in the single-run setting, because ESceme does not introduce any extra time or steps before following an instruction. Very different from pre-exploration updating the parameters of a model in unseen environments before solving the task, ESceme only renews its episodic memory while conducting instructions and does not finetune the agent. Moreover, ESceme neither involves beam search nor changes the local action space, i.e., the agent is still limited

to selecting from physically adjacent nodes at the current location. Our contributions are summarized as follows:

- We devise the first navigation mechanism with episodic scene memory (ESceme) for VLN to balance generalization and efficiency.
- We provide a simple yet effective implementation of ESceme via candidate enhancing, tested with two navigation architectures and two inferring strategies.
- We verify the superiority of ESceme in short-horizon (R2R), long-horizon (R4R), and vision-and-dialog (CVDN) navigations, and achieve a new state-of-the-art.

2 Related work

2.1 Vision-and-language navigation

Since Anderson *et al.* [3] defined the VLN task and provided an LSTM-based sequence-to-sequence baseline (Seq2Seq), numerous approaches have been developed. A branch of methods improves navigation via data augmentation, such as SF [13], EnvDrop [34], and EnvEdit [21]. As for agent training, Wang *et al.* [39] model the environment to provide planned-ahead information during navigation. RCM [38] provides an intrinsic reward for reinforcement learning via an instruction-trajectory matching critic. Wang *et al.* [40] jointly train an agent on VLN and vision-dialog navigation (MT-RCM+EnvAg). To fully use available semantic information in the environment, AuxRN [44] devises four self-supervised auxiliary reasoning tasks. TD-STP [43] introduces an extra target location estimation during finetuning to achieve reliable path planning. Many methods explore more effective feature representations and architectures, such as PTA [10], OAAM [30], NvEM [1], RelGraph [15], MTVM [24], and SEvol [6].

Inspired by the breakthrough of large-scale pre-trained BERT [19] in natural language processing tasks, PRESS [22] replaces RNNs with pre-trained BERT to encode instructions and achieves a non-trivial improvement in unseen environments. PREVELENT [14] pre-trains BERT from scratch using image-text-action triplets and further boosts the performance. RecBERT [16] integrates a recurrent unit into a BERT model to be time-aware. Chen *et al.* [7] propose the first VLN network that allows a sequence of historical memory and can be optimized end-to-end (HAMT). HOP [32] designs trajectory order modeling and group order modeling tasks to model temporal order information in pre-training. CSAP [41] proposes trajectory-conditioned masked fragment modeling and contrastive semantic-alignment modeling tasks for pre-training. ADAPT [23] explicitly learns action-level modality alignment with action prompts. There are also some works specially designed for vision-and-dialog navigation, such as VISITRON [33], SCoA [45], and CMN [46].

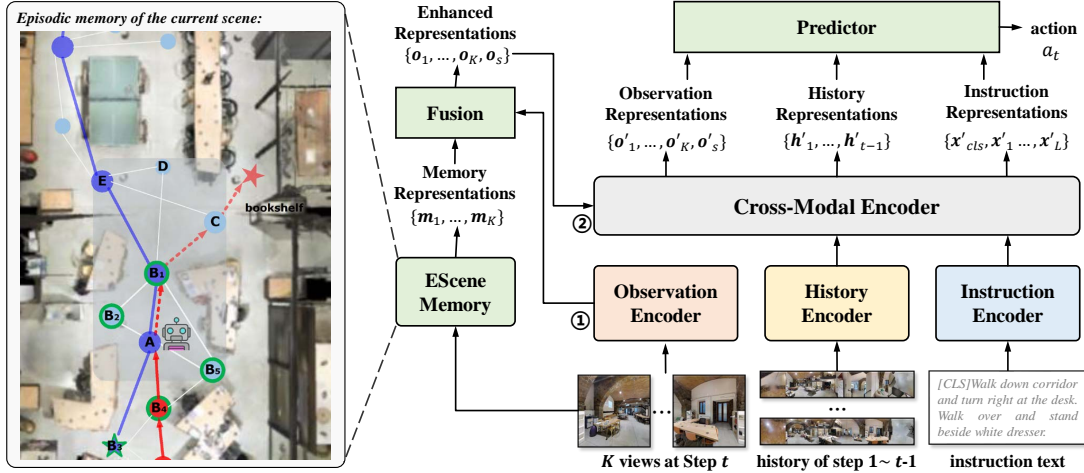


Figure 2. An overview of the **Episodic Scene** memory mechanism for VLN. On the left is partial episodic memory for the current scene, which gets updated in navigation 1) following the previous instruction, i.e. the blue route, and 2) following the current instruction from Step 1 to $t-1$, i.e. the solid red trajectory. The cyan nodes are those viewed but not visited. The shadow box shows the memory of node B_1 , which has six adjacent neighbors, i.e. A, B_2 , B_5 , C, D, and E. The integration of these nodes consists of the memory of B_1 . At Step t , the agent stands at Node A and is expected to choose one node from B_1 to B_5 . Given observation from K views, each view retrieves its memory in EScene and produces $\{m_1, \dots, m_K\}$. The memory representation then fuses with original encoded observations, which yields $\{o_1, \dots, o_K, o_s\}$. o_s is the representation for STOP. The enhanced observations, instruction text, and history from Step 1 to $t-1$ compose the input to a navigation network to predict the action $a_t = i \in \{1, \dots, K, s\}$. Generally, a navigation network uses the encoded features of the original K views as the input to the cross-modal encoder, i.e. the output ①. Our EScene exploits the enhanced observations from ②.

2.2 Exploration strategies in VLN

As the navigation graph is pre-defined in discrete VLN, diverse strategies are adopted other than the regularly used single-run. For example, Fried *et al.* [13] modify the standard beam search to select the final navigation route, which notably increases navigation success at the cost of unbearable trajectory lengths. More efficient pre-exploration methods are studied. For instance, a progress monitor is trained to discard unfinished trajectories during inference [25]. Ma *et al.* [26] learn a regret module to decide when to backtrack. Ke *et al.* [18] compare partial paths with global information considered and backtrack only when necessary. AcPercep [37] learns an exploration policy to gather visual information for navigation. Although these methods improve searching efficiency, they heavily depend on manually designed or heuristic rules. Deng *et al.* [11] define a global action space for the first time and build a graphical representation of the environment for elegant exploration/backtracking. Wang *et al.* [36] extend EnvDrop [34] with an external structured scene memory (SSM) to promote exploration in the global action space.

Pre-exploration, which allows an agent to pre-explore unseen environments before navigating, is first introduced in [38] as a setting different from single-run and beam search. The obtained information functions in diverse ways. RCM [38] uses the exploration experience in self-supervised imitation learning. EnvDrop [34] exploits the

environment information for data augmentation via back-translation. VLN-BERT [27] provides the agent with a global view for optimal route selection. AuxRN [44] fine-tunes the agent in unseen environments with auxiliary tasks.

3 Method

3.1 Problem formulation

For a specific VLN task, there is a set of training samples $\mathcal{D} = \{(Y_1, X_1, R_1), \dots, (Y_{N_1}, X_{N_1}, R_{N_1})\}$, where (X_i, R_i) is the instruction-route pair in an environment Y_i . The set $\{Y_1, \dots, Y_{N_1}\}$ composes the seen environments during training. An agent is expected to learn navigation with \mathcal{D} and carry out instructions in unseen scenarios given by $\mathcal{D}^u = \{(Y_1^u, X_1), \dots, (Y_{N_2}^u, X_{N_2})\}$. The set $\{Y_1^u, \dots, Y_{N_2}^u\}$ composes the unseen environments for test.

Given an instruction X_i , e.g. “*Turn around and walk to the right of the room...*”, an agent starts from the initial location of R_i . It observes a panoramic view of the environment Y_i . The panoramic view consists of $K=36$ single viewpoints, each of which is accompanied by an orientation (θ, ϕ) indicating heading and elevation and a binary navigable signal. The agent selects a viewpoint from the navigable ones and moves to the next location with new observations. This process repeats until the agent takes the STOP action.

For a sequence prediction problem, history is an important source of information apart from observations and in-

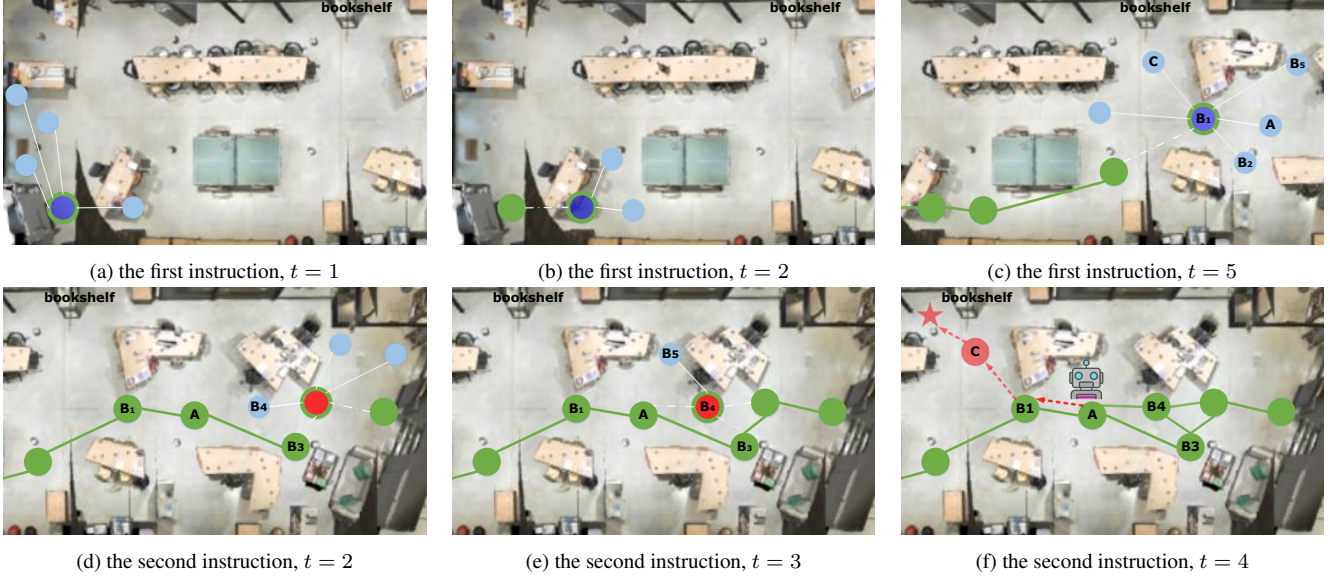


Figure 3. Episodic memory construction of a scene during navigation. ESceme at the beginning of each time step is presented in the figures, which comprises green nodes and edges and is empty at the beginning of $t = 1$. The blue nodes indicate the current location of following the first instruction at each time step, and the red ones correspond to the second instruction. The small cyan nodes mark the remaining navigable viewpoints of the current location. Nodes with green boundary are the chosen viewpoint in each time step. ESceme at the end of that time step is updated by the node with green boundary and the dashed lines connected to its existing nodes. Please refer to Figure 1 for a complete global graph of the scene, which is unavailable to the agent either in navigation or ESceme construction.

structions. The right part of Figure 2 shows a decision step by a general navigation network following the pretraining-finetuning branch that encodes path history. We denote the vanilla features of K single views extracted by the observation encoder as $\{\mathbf{f}_1, \dots, \mathbf{f}_K, \mathbf{f}_s\}$, which can be an integration of encoded RGB images and orientations. \mathbf{f}_s is appended to allow a STOP action. Together with history representations $\{\mathbf{h}_1, \dots, \mathbf{h}_{t-1}\}$ from the history encoder and text representations $\{\mathbf{x}_{cls}, \mathbf{x}_1, \dots, \mathbf{x}_L\}$ from the instruction encoder, the features of the observations ① are input into a cross-modal encoder for multi-modal fusion. A predictor block takes in the cross-modal representations $\{\mathbf{o}'_1, \dots, \mathbf{o}'_K, \mathbf{o}'_s\}$, $\{\mathbf{h}'_1, \dots, \mathbf{h}'_{t-1}\}$, and $\{\mathbf{x}'_{cls}, \mathbf{x}'_1, \dots, \mathbf{x}'_L\}$ to predict action a_t .

Due to the difference between $\{Y_1, \dots, Y_{N_1}\}$ and $\{Y_1^u, \dots, Y_{N_2}^u\}$, an agent trained in the above way suffers from decreased decision ability. The mistake accumulates along the path, which incurs a heavy drop in successful navigation in new environments. Since strategies such as pre-exploration and beam search that exploit extra clues in a new scene are too expensive for a deployed robot, we propose a mechanism of episodic scene memory to balance accuracy and efficiency. Figure 2 provides an overview of the proposed ESceme mechanism. By retrieving episodic memory for the K views at Step t , ESceme replaces the vanilla encoded observations with enhanced representations for cross-modal encoding and action prediction, i.e. ① \rightarrow ②. In the following sections, we detail how to build the episodic

scene memory and promote observations with the memory in navigation.

3.2 Episodic scene memory construction

We initialize the episodic memory of Scene Y with an empty graph $\mathcal{G}_Y^{(0)} = (\mathcal{V}_Y^{(0)} = \emptyset, \mathcal{E}_Y^{(0)} = \emptyset)$ if an agent never sees the scene. Namely, for the first instruction in Scene Y , an agent starts navigation with an empty episodic memory. As shown in Figure 3a, the start location has four neighbors and is added to \mathcal{G}_Y at the end of $t=1$ by $\mathcal{V}_Y^{(1)} = \{V_1\}$. Node feature \mathbf{m}_{V_1} is an integration of its neighbors,

$$\mathbf{m}_{V_1} = \text{pooling}(\mathbf{f}_{V_{1,i}}), \quad (1)$$

where $i \in \{1, 2, 3, 4\}$ in Figure 3a, $\mathbf{f}_{V_{1,i}} \in \mathbb{R}^d$ is d -dim plain representations of the i -th neighbor view from the observation encoder, and $\mathbf{m}_{V_1} \in \mathbb{R}^d$. The pooling function can be either *max* or *mean* pooling along the number of features. It is worth noting that obtaining $\mathbf{f}_{V_{1,i}}$ does not involve extra computation since these features have been calculated in offline feature extraction. The agent selects its right neighbor to navigate, and at the end of $t=2$, the visited node is added to \mathcal{G}_Y by $\mathcal{V}_Y^{(2)} = \{V_1, V_2\}$, $\mathcal{E}_Y^{(2)} = \{e_{12}\}$, with node feature \mathbf{m}_{V_2} calculated similarly as Eq. (1). We set all edges $e_{jk} = 1$.

While following the first instruction, the agent updates its episodic scene memory \mathcal{G}_Y accordingly, i.e. the green

nodes and edges in Figures 3b and 3c. At the end of $t = 5$, $\mathcal{V}_Y^{(5)} = \{V_1, V_2, \dots, V_5\}$, $\mathcal{E}_Y^{(5)} = \{e_{12}, e_{23}, e_{34}, e_{45}\}$. When the agent is directed to the second instruction in Scene Y , its memory in previous visits is preserved in \mathcal{G}_Y and is updated at the end of each time step accordingly as Figures 3d and 3e demonstrate. In Figure 3f, since the agent’s location A has been added to ESceme in conducting the first instruction, there is no update to \mathcal{G}_Y . The agent stores episodic memory for each scene separately in similar ways. Therefore, we omit the subscript Y for simplicity.

3.3 ESceme-assisted navigation: candidate enhancing

At each step, except for information from instruction, current observation, and route history, an agent can refer to its episodic scene memory in decision-making. Intuitively, the memory can be added to the cross-modal encoder in a separate branch. We empirically find that such a naive solution with an extra graph encoder does not promote navigation as expected. We denote the solution as Graph Encoding (GE) and provide experimental results in ablation studies. An elaboration of GE is in the supplementary material.

Since the node representation in ESceme integrates information within the neighborhood, it is expected to envision the agent with a bigger picture of the current location. Therefore, we devise a candidate-enhancing (CE) mechanism to improve navigation. A flowchart of CE is shown in Figure 2. Faced with K candidate views at Step t , the agent retrieves their representations \mathbf{m}_k , $k \in \{1, \dots, K\}$ from episodic memory $\mathcal{G}^{(t-1)}$,

$$\mathbf{m}_k = \begin{cases} \mathbf{m}_{V_j} & \text{if the } k\text{-th view is } V_j \in \mathcal{V}^{(t-1)} \\ \mathbf{0} & \text{otherwise.} \end{cases} \quad (2)$$

Then the Fusion block integrates the ESceme representations with the plain features $\{\mathbf{f}_1, \dots, \mathbf{f}_K\}$ to produce enhanced candidate viewpoints,

$$\mathbf{o}_k = \text{MLP}([\mathbf{m}_k; \mathbf{f}_k]), \quad (3)$$

where $[\cdot; \cdot]$ denotes concatenation along feature dimension. The MLP function is a two-layer non-linear projection from \mathbb{R}^{2d} to \mathbb{R}^d . Following [7, 43], type embedding that distinguishes visual and linguistic signals, navigable embedding that indicates the navigability of each candidate view, and orientation encoding are added to \mathbf{o}_k . A zero vector $\mathbf{o}_s \in \mathbb{R}^d$ is appended as the feature for STOP action.

Finally, together with encoded history features, the enhanced candidate representations $\{\mathbf{o}_1, \dots, \mathbf{o}_K, \mathbf{o}_s\}$ are input to the cross-modal encoder to merge linguistic information from encoded text features. The agent predicts the distribution of action a_t via a two-layer non-linear Predictor block,

$$P(a_t=k \in \{1, \dots, K, s\}) = \frac{e^{\mathbf{o}'_k \odot \mathbf{x}'_{cls}}}{\sum_{j \in \{1, \dots, K, s\}} e^{\mathbf{o}'_j \odot \mathbf{x}'_{cls}}}, \quad (4)$$

where \odot is element-wise multiplication. Following [34, 7], we train the framework end-to-end by a mixture of Imitation Learning and Reinforcement Learning (A2C [29]) loss,

$$\mathcal{L} = -\alpha \sum_{t=1}^{T^*} \log P(a_t=a_t^*) - \sum_{t=1}^T \log P(\tilde{a}_t)(r_t - v_t), \quad (5)$$

where T^* and T are the length of the annotated route and predicted path, respectively. \tilde{a}_t is sampled action. r_t is the discount reward, and v_t is the state value given by a two-layer (MLP) critic network.

4 Experiments

4.1 Experimental setup

Datasets and metrics. We conduct experiments on the following three VLN tasks for evaluation.

- (1) Short-horizon with fine-grained instructions. R2R [3] constructs on Matterport3D [5] and has 7,189 direct-to-goal trajectories with an average of 10m. Each path is associated with three instructions of 29 words on average. The train, val seen, val unseen, and test unseen splits include 61, 56, 11, and 18 houses, respectively.
- (2) Long-horizon with fine-grained instructions. R4R [17] is generated by joining existing trajectories in R2R with others that start close by where they end. Compared to R2R, it has longer paths and instructions and reduced shortest-path bias. The train, val seen, and val unseen have 233,613, 1,035, and 45,162 samples, respectively.
- (3) Vision-dialog navigation. CVDN [17] requires an agent to navigate given a target object and a dialog history. It has 7k trajectories and 2,050 navigation dialogs, where the paths and language contexts are also longer than those in R2R. The train, val seen, val unseen, and test splits contain 4,742, 382, 907, and 1,384 instances, respectively.

Following standard criteria [7, 3, 2], we evaluate on the R2R dataset with Trajectory Length (TL), Navigation Error (NE), Success Rate (SR), and Success weighted by Path Length (SPL). TL is the average length of an agent’s navigation route in meters, NE is the mean shortest path distance between the agent’s stop location and the target, and SR measures the ratio of navigations that stop less than three meters from the goal. SPL normalizes SR by the ratio between the path length of ground truth and the navigated, which balances accuracy and efficiency and becomes the key metric for the R2R dataset. We adopt three additional metrics, Coverage weighted by Length Score (CLS),

normalized Dynamic Time Warping (nDTW), and Success weighted by nDTW (SDTW), to assess path fidelity on the R4R dataset. As for vision-dialog navigation on CVDN, the primary evaluation metric is Goal Progress (GP) in meters. **Implementation details.** We adopt the encoders from HAMT [7] in comparison by default, where the text, history, and cross-modal encoders have nine, two, and four transformer layers, respectively. Features of single views are extracted offline using finetuned ViT-B/16 released by [7]. For a fair comparison, we set the feature dimension $d=768$, the ratio of imitation learning loss $\alpha=0.2$, and train the ESceme framework for 100K iterations on each dataset with a batch size of 8 and a learning rate of 1e-5. All the experiments run on a single NVIDIA V100 GPU. We adopt max pooling and single-run by default in comparison with other methods, and provide the results of mean pooling and inferring twice in ablation studies and supplementary material, with qualitative examples and failure cases included.

4.2 Comparison to state-of-the-art

Results on R2R dataset. Table 1 compares the proposed ESceme with existing methods on R2R dataset. We can see that the pretraining-finetuning paradigm (e.g. RecBERT [16], HAMT [7], ADAPT [23], CSAP [41], TDSTP [43]) largely improves the performance of VLN in unseen environments. ESceme achieves the highest SPL on all three splits. It surpasses the baseline model HAMT [7] by about 5% SPL on the validation and test unseen environments and even outperforms TDSTP [43] that involves auxiliary training tasks. Besides, ESceme brings a relative decrease of 6.4% and 4.1% in NE on validation and test unseen split, respectively. The results demonstrate the efficacy of episodic scene memory in generalization to unseen scenarios with short instructions.

Results on R4R dataset. We evaluate the proposed ESceme on the R4R dataset to examine if the generalization promotion maintains in long-horizon navigation tasks. The results are listed in Table 2. Our ESceme outperforms existing state-of-the-art by a large margin, i.e. a relative improvement of 6.4% in SPL, 7.0% in CLS, 7.3% in nDTW, and 9.1% in SDTW. It indicates that ESceme improves not only navigation success but also path fidelity. Although good at carrying out short instructions, TDSTP [43] suffers a heavy drop in long-horizon navigation regarding path fidelity compared with its baseline model HAMT [7]. It reveals that goal-related auxiliary tasks such as target prediction benefit reaching the target location but undermine the ability to follow instructions. Equipped with ESceme, an agent has a promoted ability to travel the expected route in long-horizon navigation. Besides, a consistent advantage of pretraining-based methods can be observed on this dataset.

Results on CVND dataset. Table 3 compares ESceme with state-of-the-art methods on the vision-and-dialog nav-

igation task. CVDN provides longer instructions and trajectories than R2R and more complicated instructions than R4R. The proposed ESceme achieves the best goal process in both seen and unseen scenarios and wins first place on the leaderboard. HAMT [7] shows an obvious advantage over other pretraining-based methods such as PREVAILENT [14], and even surpasses those counterparts specially designed for vision-and-dialog navigation, e.g. CMN [46], VISITRON [33], and SCoA [45]. Our ESceme brings a relative improvement of 20.7%, 5.7%, and 7.3% over the baseline HAMT [7] in val seen, val unseen, and test unseen environments, respectively.

4.3 Ablation studies & analysis

Different ESceme constructions. We evaluate the superiority of candidate enhancing over graph encoding and the effect of different pooling functions in Table 4. First, the graph encoding with mean pooling slightly decreases navigation success in seen environments with almost no promotion in unseen scenarios. We assume that the graph encoding adjusts the representation of observations in cross-modal encoding and does not align well with the remaining branches, resulting in a limited effect. The candidate enhancing with mean pooling brings a relative improvement of 2.3% in SPL for unseen navigation and behaves similarly in seen environments. Combined with max pooling, candidate enhancing reduces the drop and further boosts the performance in unseen environments, which produces a 3.8% relative increase compared to the HAMT [7] baseline. The results demonstrate the efficacy of the candidate enhancing and the max pooling. The candidate enhancement improves observation representations via direct injection and fusion, and the max pooling preserves more distinguishable features of each viewpoint.

Different navigation architectures & inferring strategies. The proposed ESceme is devised to be model-agnostic and should be compatible with any navigation network that has an observation input. To validate this property, we build ESceme upon TDSTP [43] that achieves the highest SR on the R2R dataset and list the results in Table 5. ESceme benefits navigation in both seen and unseen environments with a relative increase of 4.9% and 1.4%, respectively.

As introduced in Section 3.3, the agent starts with an empty episodic scene memory during inference, and the memory keeps updating. If we let the agent renew its memory in the first inference and evaluate navigation performance with a second run, it can use a much more complete episodic memory. We present the results of inferring twice in Table 5. The second inference further boosts the performance in unseen environments by 1.3% and 2.1% regarding SPL for ESceme upon HAMT [7] and TDSTP [43], respectively. More results of inferring twice are in supplementary

Method	Validation Seen				Validation Unseen				Test Unseen			
	TL	NE↓	SR↑	SPL↑	TL	NE↓	SR↑	SPL↑	TL	NE↓	SR↑	SPL↑
Seq2Seq [3]	11.33	6.01	39	-	8.39	7.81	22	-	8.13	7.85	20	18
SF [13]	-	3.36	66	-	-	6.62	35	-	14.82	6.62	35	28
AcPercep [37]	19.7	3.20	70	52	20.6	4.36	58	40	21.6	4.33	60	41
PRESS [22]	10.57	4.39	58	55	10.36	5.28	49	45	10.77	5.49	49	45
SSM [36]	14.7	3.10	71	62	20.7	4.32	62	45	20.4	4.57	61	46
EnvDrop [34]	11.00	3.99	62	59	10.70	5.22	52	48	11.66	5.23	51	47
OAAM [30]	10.20	-	65	62	9.95	-	54	50	10.40	-	53	50
AuxRN [44]	-	3.33	70	67	-	5.28	55	50	-	5.15	55	51
PREVALENT [14]	10.32	3.67	69	65	10.19	4.71	58	53	10.51	5.30	54	51
RelGraph [15]	10.13	3.47	67	65	9.99	4.73	57	53	10.29	4.75	55	52
NvEM [1]	11.09	3.44	69	65	11.83	4.27	60	55	12.98	4.37	58	54
NvEM+SEvol [6]	11.97	3.56	67	63	12.26	3.99	62	57	13.40	4.13	62	57
CSAP [41]	11.29	2.80	74	70	12.59	3.72	65	59	13.30	4.06	62	57
RecBERT [16]	11.13	2.90	72	68	12.01	3.93	63	57	12.35	4.09	63	57
ADAPT [23]	11.39	2.70	74	69	12.33	3.66	66	59	13.16	4.11	63	57
HOP [32]	11.26	2.72	75	70	12.27	3.80	64	57	12.68	3.83	64	59
TDSTP [43]	-	2.34	77	73	-	3.22	70	63	-	3.73	67	61
HAMT [7]	11.15	2.51	76	72	11.46	3.62	66	61	12.27	3.93	65	60
ESceme (Ours)	10.65	2.57	76	73	10.80	3.39	68	64	11.89	3.77	66	63

Table 1. Comparison with state-of-the-art methods on R2R dataset. ESceme (Ours) is built with HAMT [7] architecture by default.

Method	NE↓	SR↑	SPL↑	CLS↑	nDTW↑	SDTW↑
SF [13]	8.47	24	12	30	-	-
EnvDrop [34]	-	29	-	34	-	9
PTA [10]	8.25	24	10	37	32	10
RCM [38]	8.08	26	21	35	30	13
SSM [36]	8.27	32	-	53	39	19
NvEM [1]	6.85	38	28	41	36	20
NvEM+SEvol [6]	6.90	39	29	41	36	20
RelGraph [15]	7.43	36	26	41	47	34
EGP [11]	8.00	30.2	-	44.4	37.4	17.5
TDSTP [43]	6.32	43.3	40.6	46.4	42.1	25.5
RecBERT [16]	6.67	43.6	-	51.4	45.1	29.9
CSAP [41]	6.21	43.0	-	58.6	51.9	31.5
HAMT [7]	6.09	44.6	40.6	57.7	50.3	31.8
ESceme (Ours)	5.84	45.6	43.2	62.7	55.7	34.7

Table 2. Comparison on the val unseen split of R4R dataset.

material, with slighter improvements observed for longer-horizon navigation. The results demonstrate that an agent learns to assist navigation with partial and persistently updated episodic memory.

Computational efficiency. We present model size, GPU usage, and time cost during inference on the R2R dataset in Table 5. Either upon HAMT [7] or TDSTP [43], the proposed ESceme brings about 1.0% extra parameters and memory occupation in GPU. In a single-run setting, ES-

Method	Val Seen	Val Unseen	Test Unseen
Seq2Seq [3]	5.92	2.10	2.35
PREVALENT [14]	-	3.15	2.44
CMN [46]	7.05	2.97	2.95
VISITRON [33]	5.11	3.25	3.11
HOP [32]	-	4.41	3.24
SCoA [45]	7.11	2.85	3.31
MT-RCM+EnvAg [40]	5.07	4.65	3.91
HAMT [7]	6.91	5.13	5.58
ESceme (Ours)	8.34	5.42	5.99

Table 3. Results of Goal Process (GP) in meters on CVDN dataset.

ceme slightly increases the computational time by 4.8% and 3.8% when built on top of HAMT and TDSTP, respectively. Depending on a structured transformer architecture and a global action space, TDSTP incurs a relative increase of 23.5% in GPU usage and 59.5% in inference time compared with HAMT. By inferring twice, ESceme further boosts navigation performance in new environments at the expense of double the time. We can see that ESceme achieves a good trade-off between efficiency and efficacy in a single run.

Order of executing instructions. Since the agent learns with dynamically updated episodic memory while conducting instructions, the order of execution has little impact on overall performance. Table 6 shows the performance of navigation with shuffled episodes on the val unseen split in all

	GE	CE	pooling	Validation Seen				Validation Unseen			
				TL	NE↓	SR↑	SPL↑	TL	NE↓	SR↑	SPL↑
HAMT [7]	-	-	-	11.02±0.10	2.52±0.10	75.0±0.9	71.7±0.7	11.72±0.34	3.63±0.05	65.7±0.7	60.9±0.7
ESceme	✓	✗	mean	11.20±0.18	2.56±0.11	75.7±0.9	72.3±0.6	11.64±0.05	3.60±0.06	65.9±0.5	60.9±0.6
ESceme	✗	✓	mean	11.13±0.16	2.59±0.09	75.1±0.7	71.9±0.6	11.49±0.27	3.50±0.03	67.1±0.5	62.3±0.5
ESceme	✗	✓	max	10.81±0.12	2.60±0.12	75.6±0.4	72.6±0.4	11.18±0.23	3.44±0.03	67.4±0.5	63.2±0.5

Table 4. Ablation studies of ESceme construction on R2R dataset. We compare the effect of graph encoding (GE) and candidate enhancing (CE), and different pooling functions. We adopt HAMT by default in ablation comparisons.

Method	Validation Seen			Validation Unseen			Params (MB)	GPU (GB)	Time (ms)
	TL	NE↓	SPL↑	TL	NE↓	SPL↑			
HAMT [7]	11.02±0.10	2.52±0.10	71.7±0.7	11.72±0.34	3.63±0.05	60.9±0.7	651.5	8.5	29.4
+ ESceme	10.81±0.12	2.60±0.12	72.6±0.4	11.18±0.23	3.44±0.03	63.2±0.5	+6.8	+0.1	+1.4
+ ESceme (infer twice)	10.77±0.13	2.58±0.12	72.8±0.4	10.89±0.14	3.35±0.05	64.0±0.4	+6.8	+0.1	+32.2
TDSTP [43]	13.09±0.37	2.42±0.08	70.9±0.7	14.28±0.44	3.22±0.09	62.1±0.6	657.2	10.5	46.9
+ ESceme	11.80±0.26	2.34±0.10	74.4±0.6	13.86±0.21	3.31±0.07	63.0±0.8	+6.8	+0.1	+1.8
+ ESceme (infer twice)	11.83±0.23	2.33±0.08	74.8±0.7	13.38±0.28	3.21±0.05	64.3±0.7	+6.8	+0.1	+50.5

Table 5. Ablation studies of navigation architectures and inferring strategies on R2R dataset. The reported GPU occupation is for a batch size of 8 during inference, and the time cost is for a single sample on average. For a scene in R2R that has 92 nodes visited on average, the maximum episode memory costs in CPU about 1.5MB.

the datasets.

(R2R)	NE↓	SPL↑	(R4R)	SPL↑	CLS↑	(CVDN)	GP↑
	3.39±0.03	63.7±0.3		43.2±0.07	62.7±0.1		5.57±0.11

Table 6. $\bar{x} \pm \sigma$ scores of shuffled episodes with five random seeds on the val unseen split of the datasets.

Success variation during inference. Figure 4 compare SPL and CLS curves of different methods to visualize the variation of navigation quality in inferring progress. On the short-horizon navigation dataset R2R, HAMT [7] oscillates around 62 and drops in the last 1/5 progress. The decrease could result from more tough samples at the end. TDSTP [43] presents a more stable oscillation around 62, owing to a global action space and an auxiliary goal-related task. Starting from a moderate navigation ability, an agent with ESceme benefits greatly from memory updates and maintains a high success rate with completed memory.

On the long-horizon VLN dataset R4R, TDSTP [43] shares a similar oscillation around 41 with HAMT [7] in SPL. TDSTP preserves a relatively more stable success rate at the cost of much lower CLS, which reveals that goal-related auxiliary task undermines the ability of instruction following. Our ESceme shows a sharp increase within the first 4/5 navigation and keeps stable since then. We attribute the excellent promotion on R4R to two reasons, 1) long-horizon navigation involves more action steps, so a slight increase in navigation ability results in a big difference in

final performance; 2) the sample density of a scene from R4R is much higher than that from the R2R dataset.

5 Conclusion

In this paper, we devise the first VLN mechanism with episodic scene memory (ESceme) and propose a simple but effective implementation via candidate enhancing. We show that an agent with ESceme exhibits an improved navigation ability in unseen environments for three VLN tasks, including short-horizon, long-horizon, and vision-and-dialog navigation. Our method outperforms the existing state-of-the-art and wins first place in the CVDN leaderboard. We hope this work can inspire further explorations on episodic memory in VLN and related fields, e.g., building the memory in continuous environments and with more advanced techniques such as neural SLAM.

A Overview

In this document, we first elaborate on the naive solution of assisting navigation by graph encoding (GE) in Section 3.3 of the main submission (Appendix B). Then we illustrate the difference in episodic memory during navigation between a single run and inferring twice and list the tested results on all three datasets (Appendix C). Finally, we provide pseudo-code implementation for the proposed ESceme

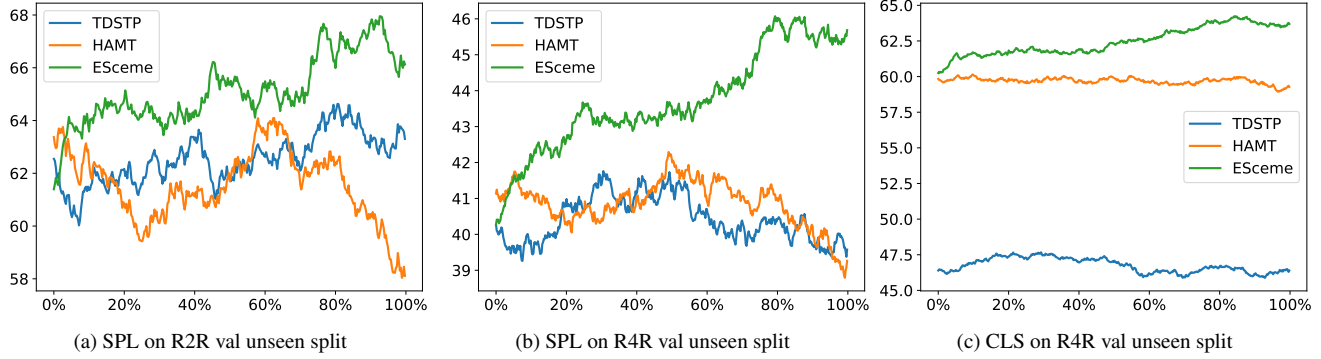


Figure 4. Navigation quality w.r.t. inferring progress. The x-axis indicates the ratio of samples tested, and the y-axis is the smoothed average of SPL or CLS. We use the default order for all the methods. Navigation with ESceme improves over time.

(Appendix D), qualitative comparisons with other methods (Appendix E), and failure cases (Appendix F).

B ESceme-assisted navigation: graph encoding

Figure 5 illustrates ESceme-assisted navigation by adding a graph encoding (GE) branch to the cross-modal encoder. At the current viewpoint that the agent stands, a local window is masked to avoid repetition with the path history from time $1 \sim t-1$. Thus, the searched episodic memory graph includes six nodes and three edges, i.e. $\mathcal{G}^{(t-1)} = \{\mathcal{V}^{(t-1)}, \mathcal{E}^{(t-1)}\}$. We adopt 3-WL GNNs [28, 12] that can distinguish two non-isomorphic graphs to encode the memory graph, where the input $G \in \mathbb{R}^{n \times n \times (1+d)}$ is given by

$$G_{ijk} = \begin{cases} e_{ij} & \text{if } k = 1 \\ m_i & \text{if } j = i \text{ for } k > 1 \\ 0 & \text{otherwise,} \end{cases} \quad (6)$$

where n is the number of nodes in $\mathcal{V}^{(t-1)}$. $m_i \in \mathbb{R}^d$ is the representation of the node V_i , with detailed calculations presented in Section 3.2 of the main submission. $e_{ij} = 1$ if V_i and V_j are connected, else $e_{ij} = 0$. The graph is encoded by

$$G' = [(W_1 G) \odot (W_2 G); (W_3 G)], \quad (7)$$

where $W_{1\sim 3} \in \mathbb{R}^{(1+d) \times (d/2)}$ are two-layer MLPs. \odot denotes element-wise multiplication and $[\cdot; \cdot]$ is concatenation along feature dimension. The final encoded feature to the cross-modal encoder is $\sum_{i=1}^n \sum_{j=1}^n G'_{ij} \in \mathbb{R}^d$.

From the results in Section 4.3 of the main submission, we can infer that encoding episodic memory in a single branch to implicitly modify the representation of observations has a limited effect on navigation.

C Single run VS. inferring twice

We provide a complete comparison between the single-run and inferring twice strategies on three datasets in Tables 7 and 8. ESceme with a second inference improves navigating in new environments by 1.6% in SPL and 2.1% in NE on test unseen split of the R2R dataset. As for vision-dialog navigation CVDN, the improvement in val unseen and test unseen are 5.5% and 3.0%, respectively. On the long-horizon navigation dataset R4R, the relative increase is less than 0.5%.

Overall, navigating by inferring twice marginally promotes generalization to new environments. The promotion is further weakened by the high sample density of scenes in CVDN, as discussed in Section 4.3 of the main submission.

D Pseudo-code implementation

We provide the pseudo-code of ESceme construction and candidate enhancing in Algorithm 1. ESceme is easy to implement and can be integrated with most navigation networks that encode the observation.

E Qualitative examples

We present the navigating process to provide a more intuitive comparison with HAMT [7] and TDSTP [43]. Figures 6 to 8 are three navigation examples on R2R dataset, and Figures 9 and 10 illustrate two examples on R4R dataset. All the examples are tested in unseen environments. For short-horizon navigation, our ESceme outperforms its counterparts regarding stopping precision. For long-horizon navigation, our ESceme shows an improved ability to follow instructions that requires a forward and back trip and arrives at the target location. We attribute these advantages to the episodic memory of the scenes.

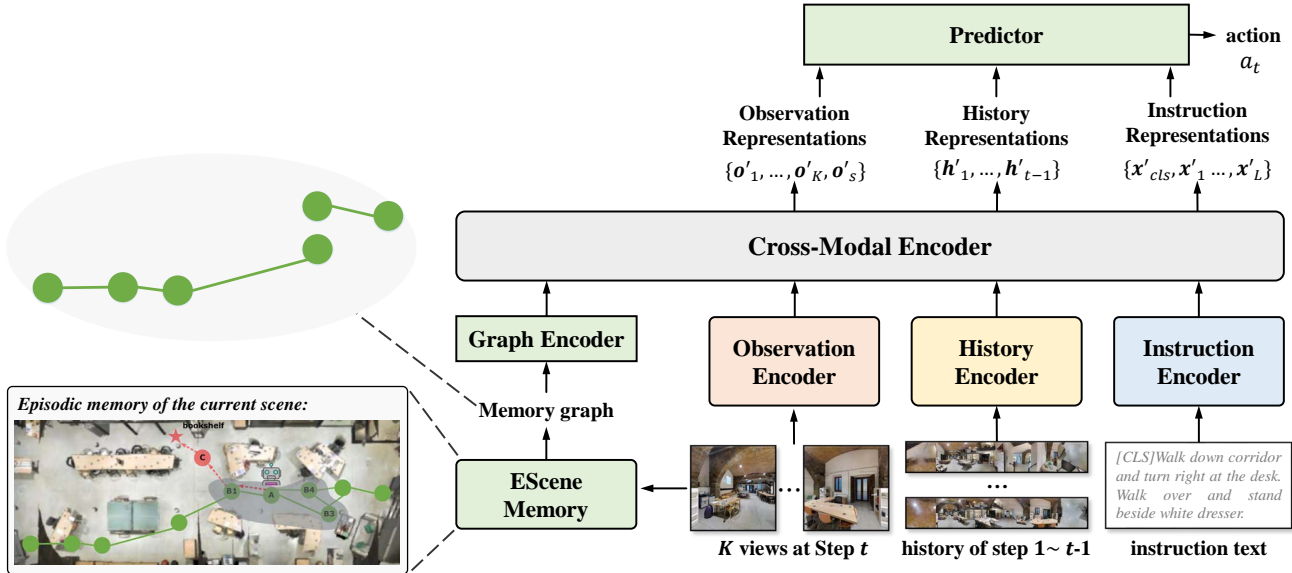


Figure 5. An overview of ESceme-assisted navigation by graph encoding. First, Episodic memory is built in the same way as that for candidate enhancing (c.f. Section 3.2 in the main submission). Then, the agent searches the episodic memory for the current viewpoint and obtains the memory graph by masking a local window. The encoded memory composes a separate branch to the cross-modal encoder.

Method	Validation Seen				Validation Unseen				Test Unseen			
	TL	NE↓	SR↑	SPL↑	TL	NE↓	SR↑	SPL↑	TL	NE↓	SR↑	SPL↑
ESceme (single run)	10.65	2.57	76	73	10.80	3.39	68	64	11.89	3.77	66	63
ESceme (infer twice)	10.62	2.57	76	73	10.65	3.36	68	64	11.77	3.69	68	64

Table 7. Results of different inferring strategies on R2R dataset.

Method	R4R Val Unseen						CVDN		
	NE↓	SR↑	SPL↑	CLS↑	nDTW↑	SDTW↑	Val Seen	Val Unseen	Test Unseen
ESceme (single run)	5.84	45.6	43.2	62.7	55.7	34.7	8.34	5.42	5.99
ESceme (infer twice)	5.83	45.8	43.4	62.9	55.8	34.8	8.39	5.72	6.17

Table 8. Results of different inferring strategies on R4R and CVDN datasets.

Algorithm 1: ESceme construction and candidate enhancing

```

def update(GY, ob):
    # GY: episodic memory of Scene Y
    # ob: observation structure that includes information of the current viewpoint and K views of a panorama
    if ob.viewpoint not in GY:
        GY.update(ob.viewpoint), feat=pooling(ob.navigable_feats)) # Update nodes by pooling ViT features
        for node in ob.navigable_views:
            if node in GY:
                GY.add.edge(ob.viewpoint, node) # Update edges
    return GY

def candidate_enhancing(GY, ob):
    m = GY.search(ob.navigable_views).feat # Search memory representations for currently navigable views
    o = MLP(torch.cat([ob.navigable_feats, m], dim=1)) # Enhance candidate representations
    o = o + embeddings # Optionally add embeddings from orientation and navigable type
    return o

```

F Failure cases

Figures 11 and 12 showcase situations where ESceme failed to following the given instructions. In the first example, the instruction is “Leave sitting room and head towards the kitchen, turn right at living room and enter. Walk through living room to dinning room and enter. Turn left and head to front door. Exit the house and stop on porch.” After correctly predicting the first three actions, ESceme failed to enter the *dinning room* and then gets lost. In the second example, the instruction is “Go down the stairs. Go into the room straight ahead on the slight left. Wait there.” ESceme succeeded in going down stairs, but failed to determine the *slight left* direction and entered the wrong room.

References

- [1] D. An, Y. Qi, Y. Huang, Q. Wu, L. Wang, and T. Tan. Neighbor-view enhanced model for vision and language navigation. In *ACMMM*, pages 5101–5109, 2021.
- [2] P. Anderson, A. Chang, D. S. Chaplot, A. Dosovitskiy, S. Gupta, V. Koltun, J. Kosecka, J. Malik, R. Mottaghi, M. Savva, et al. On evaluation of embodied navigation agents. *arXiv preprint arXiv:1807.06757*, 2018.
- [3] P. Anderson, Q. Wu, D. Teney, J. Bruce, M. Johnson, N. Sünderhauf, I. Reid, S. Gould, and A. Van Den Hengel. Vision-and-language navigation: Interpreting visually-grounded navigation instructions in real environments. In *CVPR*, pages 3674–3683, 2018.
- [4] S. Antol, A. Agrawal, J. Lu, M. Mitchell, D. Batra, C. L. Zitnick, and D. Parikh. Vqa: Visual question answering. In *ICCV*, pages 2425–2433, 2015.
- [5] A. Chang, A. Dai, T. Funkhouser, M. Halber, M. Niessner, M. Savva, S. Song, A. Zeng, and Y. Zhang. Matterport3d: Learning from rgbd data in indoor environments. In *International Conference on 3D Vision*, pages 667–676, 2017.
- [6] J. Chen, C. Gao, E. Meng, Q. Zhang, and S. Liu. Reinforced structured state-evolution for vision-language navigation. In *CVPR*, pages 15450–15459, 2022.
- [7] S. Chen, P.-L. Guhur, C. Schmid, and I. Laptev. History aware multimodal transformer for vision-and-language navigation. In *NeurIPS*, volume 34, pages 5834–5847, 2021.
- [8] S. Chen, P.-L. Guhur, M. Tapaswi, C. Schmid, and I. Laptev. Think global, act local: Dual-scale graph transformer for vision-and-language navigation. In *CVPR*, pages 16537–16547, 2022.
- [9] X. Chen, H. Fang, T.-Y. Lin, R. Vedantam, S. Gupta, P. Dollár, and C. L. Zitnick. Microsoft coco captions: Data collection and evaluation server. *arXiv preprint arXiv:1504.00325*, 2015.
- [10] F. L. L. B. M. Cornia and M. C. R. Cucchiara. Perceive, transform, and act: Multi-modal attention networks for vision-and-language navigation. *arXiv preprint arXiv:1911.12377*, 2019.
- [11] Z. Deng, K. Narasimhan, and O. Russakovsky. Evolving graphical planner: Contextual global planning for vision-and-language navigation. In *NeurIPS*, volume 33, pages 20660–20672, 2020.
- [12] V. P. Dwivedi, C. K. Joshi, T. Laurent, Y. Bengio, and X. Bresson. Benchmarking graph neural networks. *arXiv preprint arXiv:2003.00982*, 2020.
- [13] D. Fried, R. Hu, V. Cirik, A. Rohrbach, J. Andreas, L.-P. Morency, T. Berg-Kirkpatrick, K. Saenko, D. Klein, and T. Darrell. Speaker-follower models for vision-and-language navigation. In *NeurIPS*, volume 31, 2018.
- [14] W. Hao, C. Li, X. Li, L. Carin, and J. Gao. Towards learning a generic agent for vision-and-language navigation via pre-training. In *CVPR*, pages 13137–13146, 2020.
- [15] Y. Hong, C. Rodriguez, Y. Qi, Q. Wu, and S. Gould. Language and visual entity relationship graph for agent navigation. In *NeurIPS*, volume 33, pages 7685–7696, 2020.
- [16] Y. Hong, Q. Wu, Y. Qi, C. Rodriguez-Opazo, and S. Gould. Vln bert: A recurrent vision-and-language bert for navigation. In *CVPR*, pages 1643–1653, 2021.
- [17] V. Jain, G. Magalhaes, A. Ku, A. Vaswani, E. Ie, and J. Baldridge. Stay on the path: Instruction fidelity in vision-and-language navigation. In *ACL*, pages 1862–1872, 2019.
- [18] L. Ke, X. Li, Y. Bisk, A. Holtzman, Z. Gan, J. Liu, J. Gao, Y. Choi, and S. Srinivasa. Tactical rewind: Self-correction via backtracking in vision-and-language navigation. In *CVPR*, pages 6741–6749, 2019.
- [19] J. D. M.-W. C. Kenton and L. K. Toutanova. Bert: Pre-training of deep bidirectional transformers for language understanding. In *NAACL*, pages 4171–4186, 2019.

Instruction: Walk out of bedroom and turn left into hall. Walk down to end of hall and turn left into bedroom. Wait there.

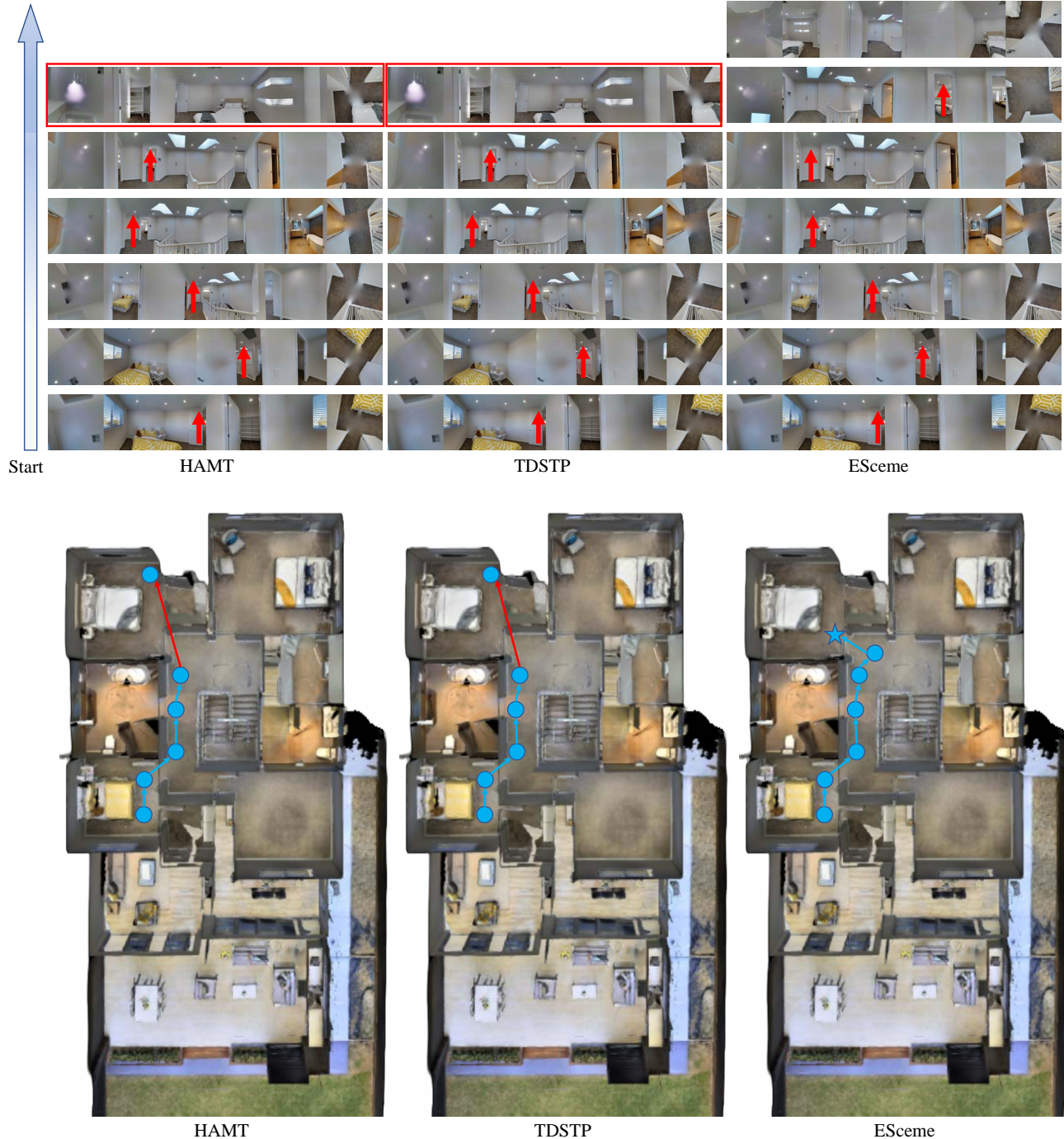


Figure 6. Panoramic views and top-down overviews of navigation. Mistakes during navigation are marked with red boxes for panorama and red arrows for top-down trajectories. The star indicates the target location. Our ESceme strictly follows the instruction “walk down to the end of hall” and waits at the door of the bedroom.

Instruction: Walk along the narrow rug past the statue on the table, and go up two steps. Wait on the third step.

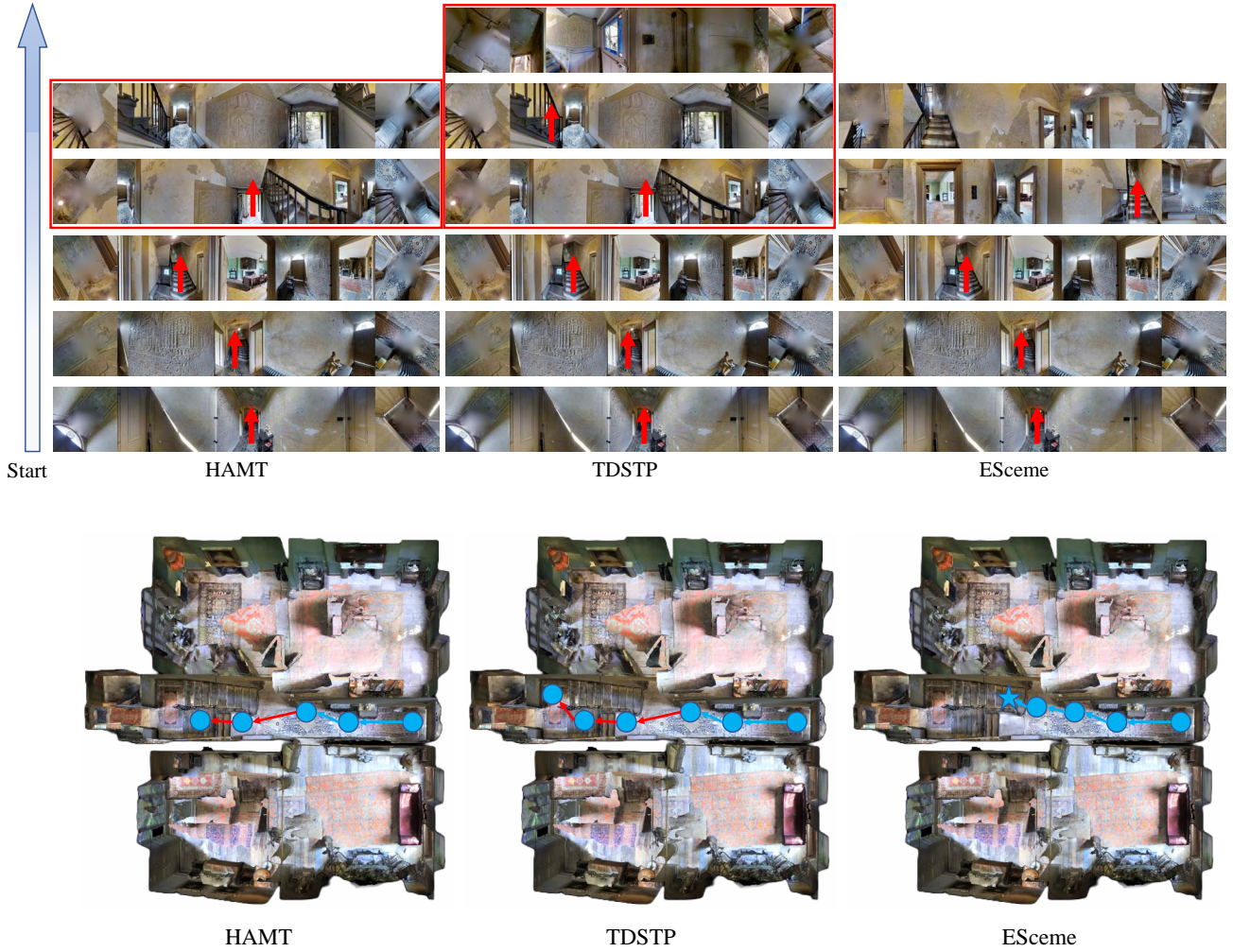


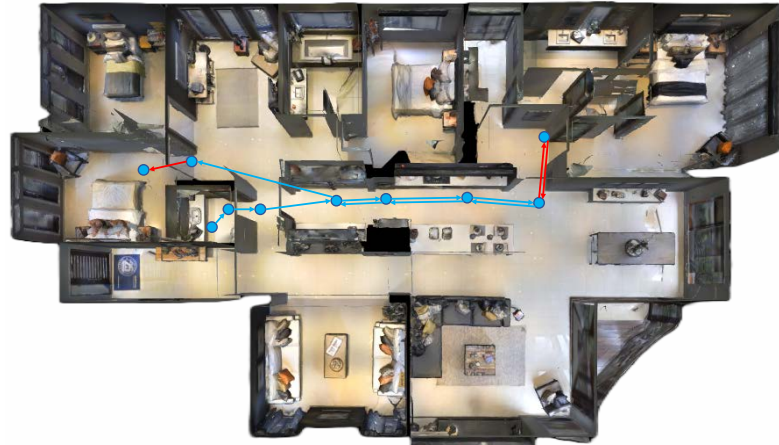
Figure 7. Panoramic views and top-down overviews of navigation. Mistakes during navigation are marked with red boxes for panorama and red arrows for top-down trajectories. The star indicates the target location. Our ESceme strictly follows the instruction “go up two steps” and waits on the third step.

Instruction: Stand with the wooden door behind you. Walk straight, past the oven and through the door to the next room. Walk through the room past the sink and microwaves. Stop after passing through the last doorway of the room with the microwaves and into the hall.

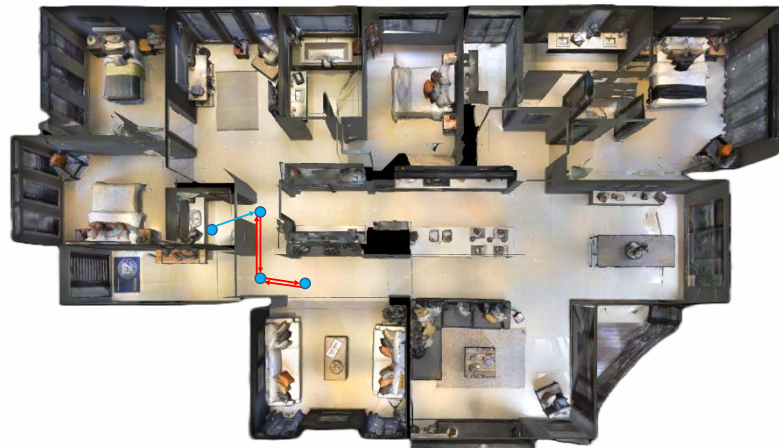


Figure 8. Panoramic views and top-down overviews of navigation. Mistakes during navigation are marked with **red** boxes for panorama and **red** arrows for top-down trajectories. The star indicates the target location. Our ESceme stops at the right place.

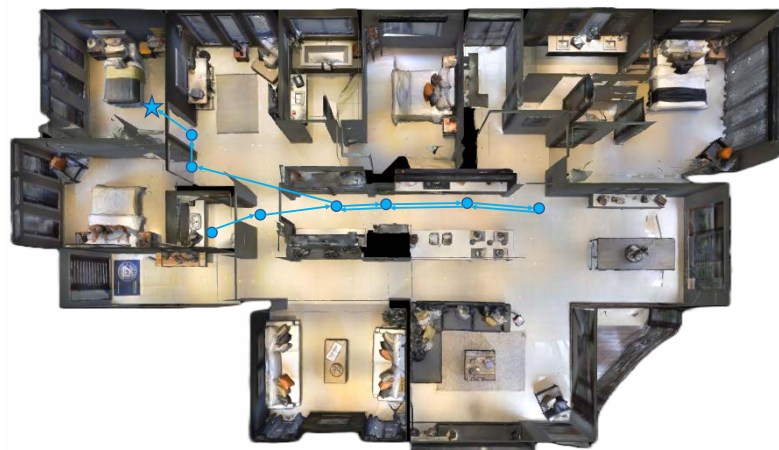
Instruction: Turn and walk out of the bathroom into the hallway. Walk through the door into the room with shelves and a sink. Continue through the room into the kitchen area and walk past the stove and sink. Turn left and walk across the kitchen hallway. When you get to a more open area, turn slight right and walk past the bedroom, then stop in the door of the second bedroom.



(a) HAMT



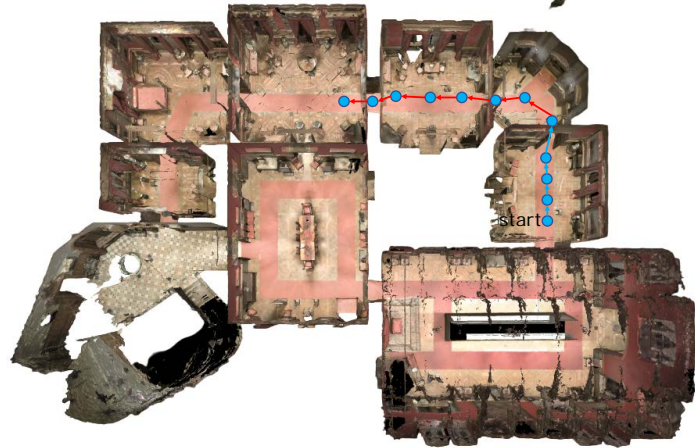
(b) TDSTP



(c) ESceme

Figure 9. The top-down trajectory of navigation. Mistakes during navigation are marked with red. The star indicates the target location. Our ESceme moves forward to the right place and then back and arrives at the second bathroom.

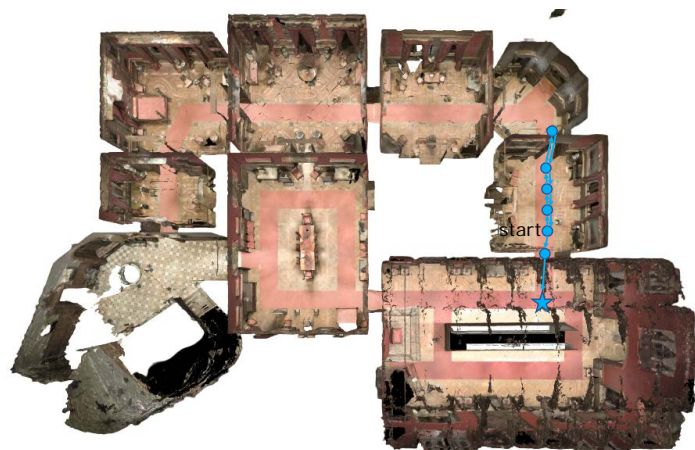
Instruction: With the desk on your left walk forward and out of this room. In the next room stop on the red rug just outside of the doorway you just left. Walk through the room and past the ropes. Stop just inside the double doors.



(a) HAMT



(b) TDSTP

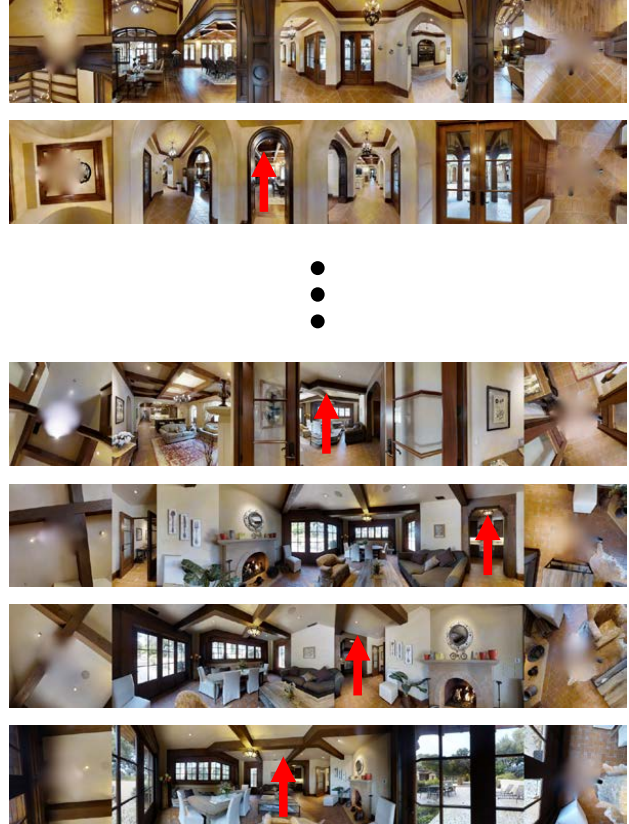


(c) ESceme

Figure 10. The top-down trajectory of navigation. Mistakes during navigation are marked with red. The star indicates the target location. Our ESceme moves forward to the right place and then back and stops inside the double doors.

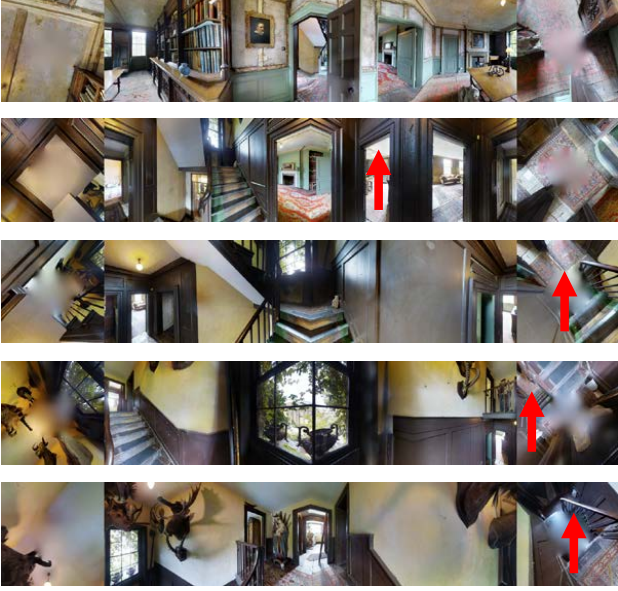


(a) ground-truth trajectory

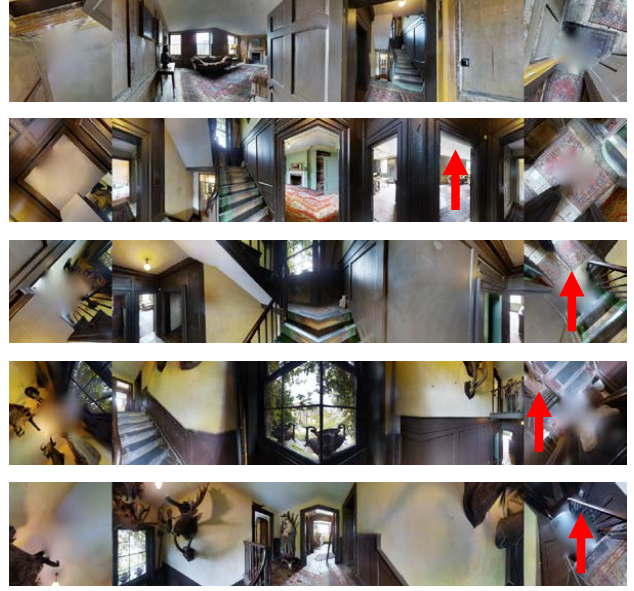


(b) trajectory predicted by ESceme

Figure 11. Failure case in R2R val unseen split. The instruction is “Leave sitting room and head towards the kitchen, turn right at living room and enter. Walk through living room to dinning room and enter. Turn left and head to front door. Exit the house and stop on porch.” After correctly predicting the first three actions, ESceme failed to enter the *dinning room* and then gets lost.



(a) ground-truth trajectory



(b) trajectory predicted by ESceme

Figure 12. Failure case in R2R val unseen split. The instruction is “Go down the stairs. Go into the room straight ahead on the slight left. Wait there.” Esceme succeeded in going down stairs, but failed to determine the *slight left* direction and entered the wrong room.

- [20] A. Ku, P. Anderson, R. Patel, E. Ie, and J. Baldridge. Room-across-room: Multilingual vision-and-language navigation with dense spatiotemporal grounding. In *EMNLP*, 2020.
- [21] J. Li, H. Tan, and M. Bansal. Envedit: Environment editing for vision-and-language navigation. In *CVPR*, pages 15407–15417, 2022.
- [22] X. Li, C. Li, Q. Xia, Y. Bisk, A. Celikyilmaz, J. Gao, N. Smith, and Y. Choi. Robust navigation with language pretraining and stochastic sampling. In *EMNLP-IJCNLP*, 2019.
- [23] B. Lin, Y. Zhu, Z. Chen, X. Liang, J. Liu, and X. Liang. Adapt: Vision-language navigation with modality-aligned action prompts. In *CVPR*, pages 15396–15406, 2022.
- [24] C. Lin, Y. Jiang, J. Cai, L. Qu, G. Haffari, and Z. Yuan. Multimodal transformer with variable-length memory for vision-and-language navigation. In *ECCV*, 2022.
- [25] C.-Y. Ma, J. Lu, Z. Wu, G. AlRegib, Z. Kira, R. Socher, and C. Xiong. Self-monitoring navigation agent via auxiliary progress estimation. In *ICLR*, 2019.
- [26] C.-Y. Ma, Z. Wu, G. AlRegib, C. Xiong, and Z. Kira. The regretful agent: Heuristic-aided navi-
- gation through progress estimation. In *CVPR*, pages 6732–6740, 2019.
- [27] A. Majumdar, A. Shrivastava, S. Lee, P. Anderson, D. Parikh, and D. Batra. Improving vision-and-language navigation with image-text pairs from the web. In *ECCV*, pages 259–274. Springer, 2020.
- [28] H. Maron, H. Ben-Hamu, H. Serviansky, and Y. Lipman. Provably powerful graph networks. *NeurIPS*, 32, 2019.
- [29] V. Mnih, A. P. Badia, M. Mirza, A. Graves, T. Lillicrap, T. Harley, D. Silver, and K. Kavukcuoglu. Asynchronous methods for deep reinforcement learning. In *ICML*, pages 1928–1937. PMLR, 2016.
- [30] Y. Qi, Z. Pan, S. Zhang, A. v. d. Hengel, and Q. Wu. Object-and-action aware model for visual language navigation. In *ECCV*, pages 303–317. Springer, 2020.
- [31] Y. Qi, Q. Wu, P. Anderson, X. Wang, W. Y. Wang, C. Shen, and A. v. d. Hengel. Reverie: Remote embodied visual referring expression in real indoor environments. In *CVPR*, pages 9982–9991, 2020.
- [32] Y. Qiao, Y. Qi, Y. Hong, Z. Yu, P. Wang, and Q. Wu. Hop: History-and-order aware pre-training for vision-and-language navigation. In *CVPR*, pages 15418–15427, 2022.

[33] A. Shrivastava, K. Gopalakrishnan, Y. Liu, R. Piramuthu, G. Tür, D. Parikh, and D. Hakkani-Tur. Vis-itrion: Visual semantics-aligned interactively trained object-navigator. In *Findings of the Association for Computational Linguistics: ACL 2022*, pages 1984–1994, 2022.

[34] H. Tan, L. Yu, and M. Bansal. Learning to navigate unseen environments: Back translation with environmental dropout. In *NAACL*, 2019.

[35] J. Thomason, M. Murray, M. Cakmak, and L. Zettlemoyer. Vision-and-dialog navigation. In *Conference on Robot Learning*, pages 394–406. PMLR, 2020.

[36] H. Wang, W. Wang, W. Liang, C. Xiong, and J. Shen. Structured scene memory for vision-language navigation. In *CVPR*, pages 8455–8464, 2021.

[37] H. Wang, W. Wang, T. Shu, W. Liang, and J. Shen. Active visual information gathering for vision-language navigation. In *ECCV*, pages 307–322. Springer, 2020.

[38] X. Wang, Q. Huang, A. Celikyilmaz, J. Gao, D. Shen, Y.-F. Wang, W. Y. Wang, and L. Zhang. Reinforced cross-modal matching and self-supervised imitation learning for vision-language navigation. In *CVPR*, pages 6629–6638, 2019.

[39] X. Wang, W. Xiong, H. Wang, and W. Y. Wang. Look before you leap: Bridging model-free and model-based reinforcement learning for planned-ahead vision-and-language navigation. In *ECCV*, pages 37–53, 2018.

[40] X. E. Wang, V. Jain, E. Ie, W. Y. Wang, Z. Kozareva, and S. Ravi. Environment-agnostic multitask learning for natural language grounded navigation. In *ECCV*, pages 413–430. Springer, 2020.

[41] S. Wu, X. Fu, F. Wu, and Z.-J. Zha. Cross-modal semantic alignment pre-training for vision-and-language navigation. In *ACMMM*, pages 4233–4241, 2022.

[42] J. Xu, T. Mei, T. Yao, and Y. Rui. Msr-vtt: A large video description dataset for bridging video and language. In *CVPR*, pages 5288–5296, 2016.

[43] Y. Zhao, J. Chen, C. Gao, W. Wang, L. Yang, H. Ren, H. Xia, and S. Liu. Target-driven structured transformer planner for vision-language navigation. In *ACMMM*, pages 4194–4203, 2022.

[44] F. Zhu, Y. Zhu, X. Chang, and X. Liang. Vision-language navigation with self-supervised auxiliary reasoning tasks. In *CVPR*, pages 10012–10022, 2020.

[45] Y. Zhu, Y. Weng, F. Zhu, X. Liang, Q. Ye, Y. Lu, and J. Jiao. Self-motivated communication agent for real-world vision-dialog navigation. In *ICCV*, pages 1594–1603, 2021.

[46] Y. Zhu, F. Zhu, Z. Zhan, B. Lin, J. Jiao, X. Chang, and X. Liang. Vision-dialog navigation by exploring cross-modal memory. In *CVPR*, pages 10730–10739, 2020.